Industrial Engineering Journal
ISSN: 0970-2555
Volume : 53, Issue 4, No. 4, April : 2024

CFD ANALYSIS OF WHALE INSPIRED HYDROFOIL AT DIFFERENT ANGLES OF ATTACK

Ratnala Prasad, Assistant Professor, Department of Mechanical Engineering, Aditya College of Engineering & Technology (A), Surampalem, AP, India-533437
K. Subrahmanya Singh B.Tech, Department of Mechanical Engineering, Aditya College of Engineering & Technology (A), Surampalem, AP, India-533437 Email: appusingh675@gmail.com
N. Naga Santosh B.Tech, Department of Mechanical Engineering, Aditya College of Engineering & Technology (A), Surampalem, AP, India-533437
K. Chandranadh B.Tech, Department of Mechanical Engineering, Aditya College of Engineering & Technology (A), Surampalem, AP, India-533437
B. Vijay Veera Naga Prasad B.Tech, Department of Mechanical Engineering, Aditya College of Engineering & Technology (A), Surampalem, AP, India-533437

Abstract
The rapid advancement in bio-inspired engineering has spurred interest in the study and application of natural designs to enhance the performance of various technologies. This project focuses on the Computational Fluid Dynamics (CFD) analysis of a hydrofoil inspired by the streamlined morphology of whale flippers. The objective is to investigate the hydrodynamic characteristics of the whale-inspired hydrofoil under different angles of attack, aiming to optimize its efficiency and maneuverability. The CFD simulations are conducted using state-of-the-art software, incorporating a three-dimensional model of the hydrofoil geometry. The numerical study explores a range of angles of attack to understand the hydrodynamic forces, lift, drag, and flow patterns around the hydrofoil. By systematically varying the angle of attack, the project aims to identify the optimal configuration that maximizes lift while minimizing drag, leading to improved hydrofoil performance.

The outcomes of this research hold potential implications for the design and development of underwater vehicles, marine propulsion systems, and other hydrodynamic applications. The insights gained from the CFD analysis provide a basis for refining the hydrofoil's design parameters and contribute to the broader field of bio-inspired engineering. The study not only advances our understanding of fluid dynamics in marine environments but also presents practical implications for the development of efficient and biomimetic hydrofoil designs.

Keywords:
Hydrofoil, Fluent, K-omega, K-epsilon, Turbulence kinetic energy

1. Introduction

Flows around marine propellers, sailboat keels or control surfaces are inherently three-dimensional. Moreover, it is even impossible to create a truly two-dimensional flow in a wind or water tunnel. While the foil model may be perfectly placed between the walls of the tunnel test section, interaction between the tunnel wall boundary layers and the foil generate three-dimensional features that disturb the two-dimensional of the flow field. Reliable experimental measurements of two-dimensional foil sections therefore require careful attention to the issue of avoiding unwanted three-dimensional effects.

Moreover, the fundamental mechanism for creating lift as well as much of the methodology for designing optimum foil section shapes can be explained by two-dimensional concepts. Design methods for airplane wings, marine propellers, and everything in between rely heavily on the use of systematic foil section data. But, it is important to recognize that one cannot simply piece together a three-dimensional wing or propeller in a strip-wise manner from a sequence of two-dimensional foil sections and expect to get an accurate answer. We will see later why this is true, and how two and three-dimensional flows can be properly combined.

A surprisingly large number of methods exist for predicting the flow around foil sections, and it is important to understand their advantages and disadvantages. They can be characterized in the following three ways, Analytical or Numerical.

The initial development of the field of airfoil theory took place in the early 1900's, long before the invention of the computer. Obtaining an accurate solution for the flow around such a complex shape as a foil section, even in two-dimensions, was therefore a formidable task. Fortunately, one analytical technique, known as the method of conformal mapping, was known at that time, and provided a means of determining the exact in- viscid flow around a limited class of foil section shapes. This technique was first applied by Joukowski in 1914, and the set of foil geometries created by the mapping function which he developed bears his name. A more general mapping function, which includes the Joukowski mapping as a special case, was then introduced by Karman and Trefftz. While other several investigators introduced different mapping functions, the next significant development was by Theodorsen, who developed an approximate analytical/numerical technique for obtaining the mapping function for a foil section of arbitrary shape.

Theodorsen's work was the basis for the development of an extensive systematic series of foil sections published by the National Advisory Commission on Aeronautics (NACA) in the late 1930's and 1940's. The old NACA section results were done, of necessity, by a combination of graphical and hand computation. An improved conformal mapping method of computing the flow around arbitrary sections, suitable for implementation on a digital computer, was developed by who found, not surprisingly, that in accuracies existed in the earlier NACA data. Brockett's work led to the development of foil section design charts which are used for propeller design at the present time.

The theoretical basis for the method of conformal mapping is given in most advanced calculus texts, so only the essential highlights will be developed here. One starts with the known solution to a simple problem in this case the flow of a uniform stream past a circle. The circle is then "mapped" into some geometry that resembles a foil section, and if you follow the rules carefully, the flow around the circle will be transformed in such a way as to represent the correct solution for the mapped foil section. Capturing the turbulence accurately has troubled the CFD community for years yet there are several ways using which one can simulate them effectively to achieve accurate aerodynamic results. Das Karmakar and Chattopadhyay (2022) evaluated several augmentation approaches and devices to improve VAWT effectiveness. The cowling technique, invelox profile, and inlet flow path modification were evaluated. The performance and structural analysis of wind turbines were comprehensively studied by Rajamohan (2022).

A considerable volume of research work had been dedicated towards investigating the influence of leading-edge protuberances on full span airfoils. Experimental results presented in (Johari, 2007) at $Re = 1.83 \times 10^5$ demonstrated the disadvantages for NACA 634–021 airfoils with tubercles in pre-stall compared to an unmodified airfoil. Similarly, experimental (Zverkov, 2008), (Kozlov, 2007) and numerical (Aftab and Ahmad, 2014) results show that the wavy wing outperforms the classical wing in the post-stall region. Numerical calculations presented in (Feng, 2012) showed that the modified foil delays the stall by around 3° compared to a normal foil.

The flow patterns governing these outcomes were studied using dye visualization experiments (Custodio, 2007) which indicated that pairs of counter-rotating streamwise vortices were generated in the troughs between tubercles at $Re = 1.8 \times 10^5$, resulting in flow attachment behind the tubercle crests in post-stall.

The idea of applying WLE on foil was firstly presented by marine biologists Fish and Battle (1995) in 1995. Following the investigations of Fish and Battle, many researchers studied the aerodynamic characteristics of the wavy leading edge foil. The aerodynamic performance capabilities of the flippers with the addition of the leading edge tubercles were studied by Miklosovic. (2004) in a wind tunnel. The presence of the tubercles delays stall to higher angle by about 40%, increases maximum lift by 6%, and decreases drag up to 32%. Their experimental were corroborated by the numerical simulation performed by Carreira Pedro and Kobayashi (2008) through the DES (Detached

Eddy Simulation) method. Guerreiro and Sousa (2012) experimentally examined the effect of Reynolds numbers on the flow over the WLE and indicated that the lift force of the WLE case is less sensitive to Reynolds numbers in comparison to the baseline model.

According to the investigation from Custodio (2007), the flow past each protuberance is periodic and symmetric at small attack angles, but when some critical attack angle is exceeded, the flow field is no longer periodic from peak to peak and valley to valley, but is now bi-periodic, this phenomenon is also reported to occur computationally by Câmara and Sousa (2013). Wei, 2015, Wei, 2019 experimentally studied leading edge tubercles performances for Re=1.4×10^4 and showed that the leading edge tubercles can mitigate flow separation and stream-wise counter-rotating vortex pairs are generated over tubercles.

Figure 1: whale inspired hydrofoil

2. Realizable k □ε turbulence model

The simplest "complete models" of turbulence are two equation models in which the solution of two separate transport equations allows the turbulent velocity and length scales to be independently determined. The standard k □ □ model falls within this class of turbulence model and has become the workhorse of practical engineering flow calculations in the time since it was proposed by Launder and Spalding (1974). Robustness, economy and reasonable accuracy for a wide range of turbulent flows explain its popularity in industrial flow and heat transfer simulations. It is a semi-empirical model and the derivation of the model equations rely on phenomenological considerations and empiricism. As the strengths and weaknesses of the standard k □ □ model have become known, improvements have been made to the model to improve its performance. Two of these variants are available: the RNG k □ □ model and the Realizable k □ □ model (Shih et al., 1995). The modelled transport equations for k and ε in the

$$\frac{\partial}{\partial t}(\rho\varepsilon)+\frac{\partial}{\partial x_j}(\rho\varepsilon u_j)=\frac{\partial}{\partial x_j}\left[\left(\mu+\frac{\mu_t}{\sigma_\varepsilon}\right)\frac{\partial\varepsilon}{\partial x_j}\right]+\rho C_1 S\varepsilon-\rho C_2\frac{\varepsilon^2}{k+\sqrt{v\varepsilon}}+C_{1\varepsilon}\frac{\varepsilon}{k}C_{3\varepsilon}G_b+S_\varepsilon$$

where

$$C_1=\max\left[0.43,\frac{n}{n+5}\right],n=S\frac{k}{\varepsilon},S=\sqrt{2S_{ij}S_{ij}}$$

In these equations, Gk represents the generation of turbulence kinetic energy due to the mean velocity gradients. Gb is the generation of turbulence kinetic energy due to buoyancy. YM represents the contribution of the fluctuating dilatation in compressible turbulence to the overall dissipation rate (2 YM

□ 2□□Mt, where M t is the turbulent Mach number). C2 and C1ε are constants. K- σ and □- σ are the turbulent Prandtl numbers for k and ε, respectively. k S and Sε are user-defined source terms.

Industrial Engineering Journal
ISSN: 0970-2555
Volume : 53, Issue 4, No. 4, April : 2024

The constants of the Realizable k □□ model is: C1□ □1.44, C2 □1.9, □ k □1.0 and □1.2 □ □ .
The standard k □□ model is based on the Wilcox (1988) k □□ model, which incorporates modifications for low

$$\frac{\mathrm{D}\rho\omega}{\mathrm{D}t}=\frac{\gamma}{\nu_t}\tau_{ij}\frac{\partial u_i}{\partial x_j}-\beta\rho\omega^2+\frac{\partial}{\partial x_j}\left[(\mu+\sigma_\omega\mu_t)\frac{\partial\omega}{\partial x_j}\right]+2\rho(1-F_1)\sigma_\omega\frac{1}{\omega}\frac{\partial k}{\partial x_j}\frac{\partial\omega}{\partial x_j}$$

Where □ □ □ k□ * and the turbulence stress tensor is

$$\tau_{ij}=-\rho\overline{u_i'u_j'}=\mu_t\left(\frac{\partial u_i}{\partial x_j}+\frac{\partial u_j}{\partial x_i}-\frac{2}{3}\frac{\partial u_k}{\partial x_k}\delta_{ij}\right)-\frac{2}{3}\rho k\delta_{ij} \quad (16)$$

The turbulence viscosity can be estimated by □ □ 1 1 2 vt □ a k max a □,□F , where □ is the absolute value realizable k □ □ model are:

$$\frac{\partial}{\partial t}(\rho k)+\frac{\partial}{\partial x_j}(\rho k u_j)=\frac{\partial}{\partial x_j}\left[\left(\mu+\frac{\mu_t}{\sigma_k}\right)\frac{\partial k}{\partial x_j}\right]+G_k+G_b-\rho\varepsilon-Y_M+S_k$$

Reynolds number effects, compressibility and shear flow spreading. The Wilcox model predicts free shear flow spreading rates that are in close agreement with measurements for far wakes, mixing layers and plane, round, and radial jets, and is thus applicable to wall bounded flows and free shear flows. A variation of the standard k □□ model called the k □□ SST model is also available. The k □□ SST model was developed by Menter (1994) to effectively blend the robust and accurate formulation of the k □□ model in the near-wall region with the free-stream independence of the k □□ model in the far field. To achieve this, the k □□ model is converted into a k □□ formulation. The k □□ SST model is similar to the standard k □□ model, but includes some refinements. These features make the k □□ SST model more accurate and reliable for a wider class of flows (for example, adverse pressure gradient flows, airfoils, transonic shock waves) than the standard k □□ model. The k □□ SST turbulence model is a combined version of the k □□ and the k □□ turbulence models and is governed by:

$$F_2=\tanh\left\{\left[\max\left(\frac{2\sqrt{k}}{0.09\omega y},\frac{500\nu}{y^2\omega}\right)\right]\right\}^2$$

Where y is the distance to the nearest surface. The coefficients k □,□ ,□ and □ □ are defined as functions of the coefficients of the k □□ and k □□ turbulence models and they are listed as follows:

$$\beta=F_1\beta_1+(1-F_1)\beta_2,\ \gamma=F_1\gamma_1+(1-F_1)\gamma_2,$$
$$\sigma_k=F_1\sigma_{k1}+(1-F_1)\sigma_{k2},\ \sigma_\omega=F_1\sigma_{\omega1}+(1-F_1)\sigma_{\omega2}$$

where the function F1 is

$$F_1=\tanh\left\{\left[\min\left[\max\left(\frac{\sqrt{k}}{0.09\omega y},\frac{500\nu}{y^2\omega}\right),\frac{4\rho\sigma_{\omega2}k}{CD_{k\omega}y^2}\right]\right]^4\right\}$$

and the coefficient CDk□ is

$$CD_{k\omega}=\max\left(2\rho\sigma_{\omega2}\frac{1}{\omega}\frac{\partial k}{\partial x_j}\frac{\partial\omega}{\partial x_j},10^{-20}\right)$$

Industrial Engineering Journal
ISSN: 0970-2555
Volume : 53, Issue 4, No. 4, April : 2024

The empirical constants of the k □□ SST model are: 0.09 * □ □ , □1 □ 0.075, □ 2 □ 0.0828, □ 1 □ 0.5532, □ 2 □ 0.4404, □ k1 □ 0.85, □ k 2 □1.0, □ □1 □ 0.5 and □ □2 □ 0.856

3. Modelling And Analysis

Space Claim is a computer-aided design (CAD) software developed by Space Claim Corporation. It is a 3D modelling software that allows users to create and edit 3D models quickly and easily. One of the main features of Space Claim is its ability to work with any geometry, regardless of where it comes from. This makes it an ideal tool for engineers, designers, and architects who need to work with data from multiple sources, including scanned data and other CAD systems.

Space Claim also includes a range of tools for creating and editing 3D models. Users can create models using a variety of techniques, including direct modelling, which allows them to modify geometry quickly and easily using push-pull operations, and parametric modelling, which allows them to create models that can be easily edited and modified later. In addition, Space Claim includes tools for creating assemblies and performing simulations, such as finite element analysis (FEA) and computational fluid dynamics (CFD). It also includes features for creating 2D drawings.

Space Claim is designed to be easy to learn and use, with an intuitive interface and a set of powerful tools that allow users to create and manipulate 3D geometry without having to be experts in traditional CAD software

Quick sketching and modelling tools that allow users to create new 3D models from scratch or modify existing ones.

Easy import/export of CAD files from a variety of different formats, including STEP, IGES, SAT, and STL.

A variety of powerful editing tools, including push-pull, move, scale, and rotate functions, as well as more advanced tools like filleting, chamfering, and shelling.

Real-time analysis tools that allow users to check the integrity and quality of their models, including tools for measuring distances, angles, and volumes

Space Claim is a solid modelling CAD software that runs on Microsoft Windows and was developed by Space Claim Corporation. The company is headquartered in Concord, Massachusetts.

Space Claim Corporation was founded in 2005 to develop 3D solid modelling software for mechanical engineering. Its first CAD application was launched in 2007 and used an approach to solid modelling where design concepts are created by pulling, moving, filling, combining, and reusing 3D shapes.

It was acquired by Ansys in May 2014, Inc, and was integrated into subsequent versions of Ansys Simulation packages as a built-in 3D modeler. Space Claim Corporation Markets Space Claim Engineer directly to end-user and indirectly by other channels. Space Claim also licenses its software for OEMs, such as ANSYS, Flow International Corporation.

Space Claim's 3D direct modelling technology is primarily expressed through its user interface in four tools: pull, move, fill, and combine:

Pull contains most creation features found in traditional CAD systems, determining its behaviour through users' selection and though the use of secondary tool guides. For example, using the Pull tool on a face by default offsets the face, but using the Pull tool on an edge rounds the edge.

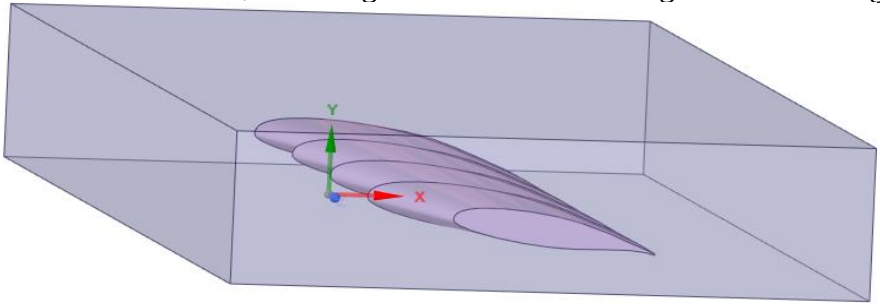

Figure 2: hydrofoil geometry

Industrial Engineering Journal
ISSN: 0970-2555
Volume : 53, Issue 4, No. 4, April : 2024

4. Results and Discussions

ANSYS is a widely-used engineering simulation software that enables engineers to analyze and design products and systems in a virtual environment. The software provides tools for structural analysis, fluid dynamics, electromagnetics, and more, allowing engineers to simulate and optimize a wide range of physical phenomena. With ANSYS, engineers can simulate the behavior of structures and components under various loads and conditions. The software provides tools for linear and nonlinear static and dynamic analysis, as well as fatigue analysis and optimization. ANSYS also supports a wide range of material models, including isotropic, anisotropic, and orthotropic materials. ANSYS allows engineers to simulate fluid flow and heat transfer in complex geometries. The software provides tools for both steady-state and transient analyses, as well as turbulence modeling and multi-phase flow. ANSYS enables engineers to simulate electromagnetic phenomena, including electromagnetic fields, electromagnetic waves, and electromagnetic devices. The software provides tools for both low-frequency and high-frequency analysis, as well as for circuit simulation and signal integrity analysis.

Meshes are used for rendering to a computer screen and for physical simulation such as finite element analysis or computational fluid dynamics as shown in figure 1. Meshes are composed of simple cells like triangles because, e.g., we know how to perform operations such as finite element calculations (engineering) or ray tracing (computer graphics) on triangles, but we do not know how to perform these operations directly on complicated spaces and shapes such as a roadway bridge. We can simulate the strength of the bridge, or draw it on a computer screen, by performing calculations on each triangle and calculating the interactions between triangles.

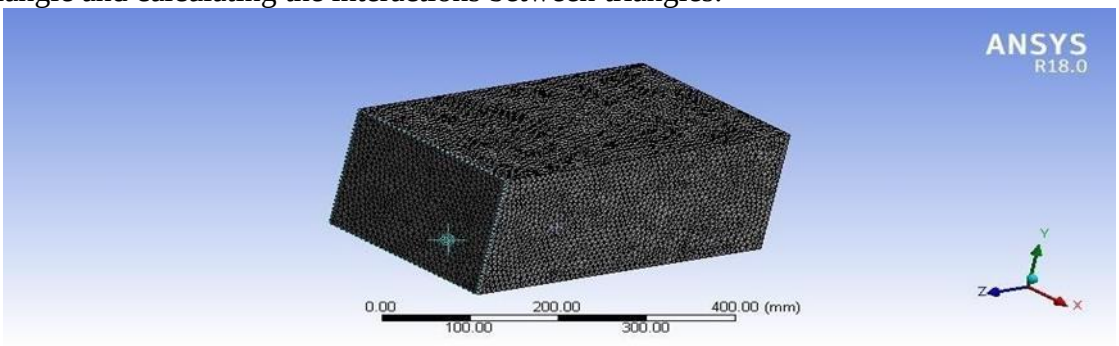

Figure 3: hydrofoil mesh

Computers are used to perform the calculations required to simulate the free-stream flow of the fluid, and the interaction of the fluid (liquids and gases) with surfaces defined by boundary conditions. With high speed super computer better solutions can be achieved, and are often required to solve the largest and most complex problems. Ongoing research yields software that improves the accuracy and speed of complex simulation scenarios such as transonic or turbulent flows .Initial validation of such software is typically performed using experimental apparatus such as wind tunnels are shown in Table 1-3. In addition, previously performed analytics or empirical analysis of a particular problem can be used for comparison. A final validation is often performed using full-scale testing, such as flight tests as shown in Figure 4.

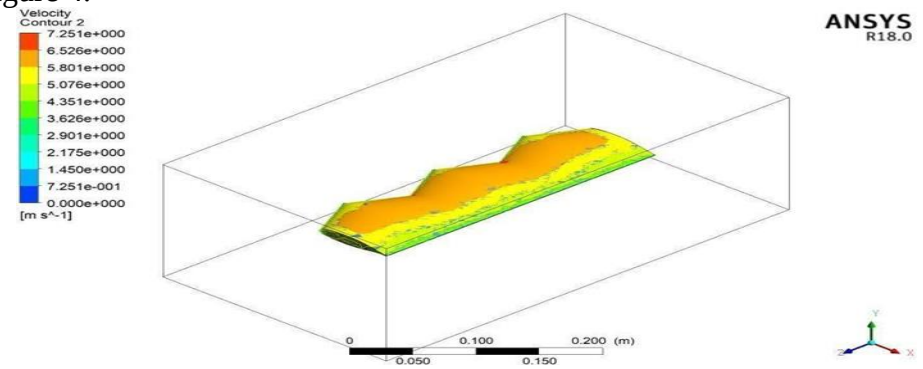

Industrial Engineering Journal
ISSN: 0970-2555
Volume : 53, Issue 4, No. 4, April : 2024

Figure 4: velocity contour for zero deg angle of attack

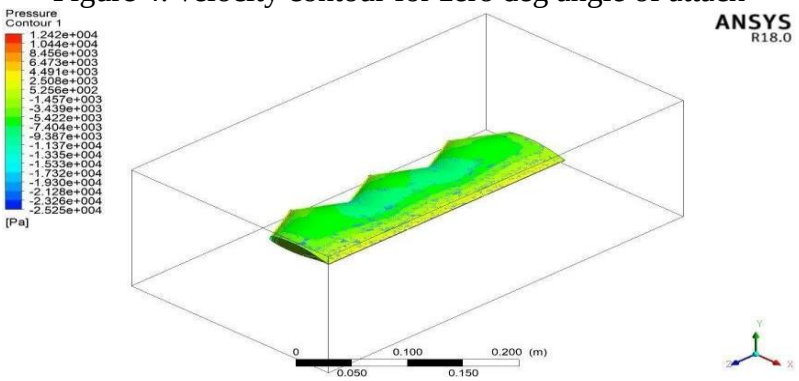

Figure 5: Pressure contour for zero deg angle of attack

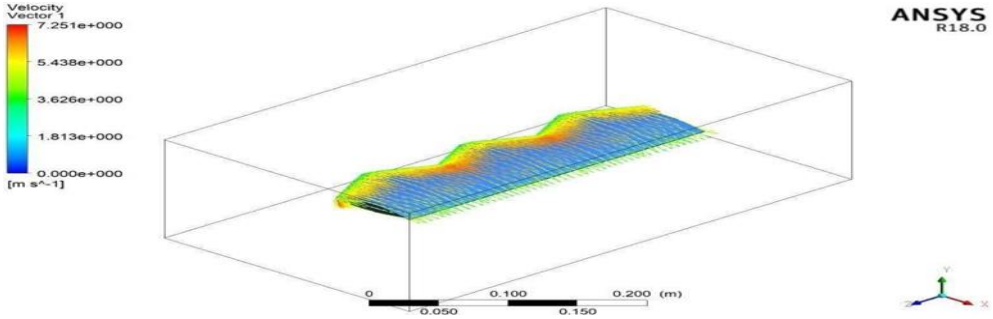

Figure 6: Velocity vectors for zero deg angle of attack

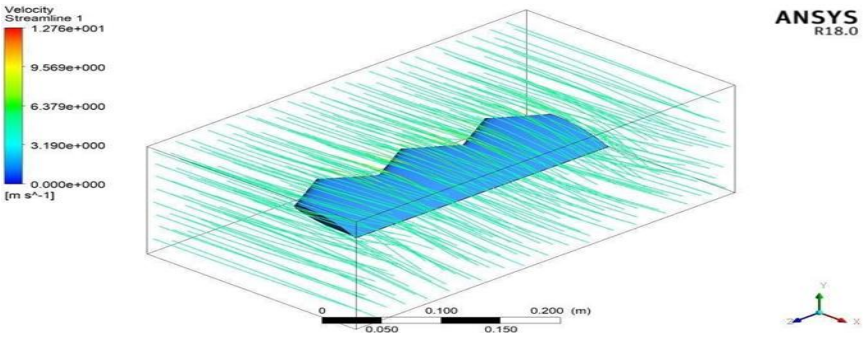

Figure 7: Velocity streamlines for 12 deg angle of attack

Table 1 Angle of attack with pressure and velocity variations

S.No	Angle of attack	Pressure variation[pa]	Velocity variations[m/s]
1	0^o	12420	7.251
2	3^o	12600	7.705
3	6^o	13090	9.152
4	9^o	13480	10.97
5	12^o	14020	12.76

Table 2 Angle of attack with lift and drag variations

Angle of Attack	Coefficient of Lift	Coefficient of Drag
0^o	0.2	0.01
3^o	0.5	0.03
6^o	0.8	0.06
9^o	1.1	0.1

12^o	1.4	0.15

Table 3 Angle of attack with lift and drag variations

Angle ofMAttack	Coefficient of Lift	Coefficient ofDrag	Lift force[N]	Drag force[N]
0^o	0.2	0.01	50	2.5
3^o	0.5	0.03	100	7.5
6^o	0.8	0.06	175	15
9^o	1.1	0.1	250	22.5
12^o	1.4	0.15	325	30

5. Conclusion

This study investigates the impact of varying angles of attack (AoA) on the performance of a whale-inspired hydrofoil through Computational Fluid Dynamics (CFD) analysis. Ranging from 0 to 12 degrees, the investigation focuses on understanding hydrodynamic forces affecting the hydrofoil. ANSYS Fluent simulations reveal that a 12-degree AoA notably enhances both pressure and velocity differentials, indicating improved lift and propulsion capabilities. This finding suggests optimal hydrofoil configurations for maximum lift and minimal drag, crucial for applications requiring increased lift and velocity. Future research could explore fluid dynamics in depth and validate results through physical prototypes, while these insights advance biomimetic engineering, emphasizing nature-inspired designs' potential for enhancing hydrofoil efficiency across diverse applications.

References

1. R.Kant, A.Bhattacharyya, “A bio-inspired twin-protuberance hydrofoil design” , Volume 218, 15 December 2020, 108209
2. Yongkuang Zhang a b, Xinyang Han a b, Yuxuan Hu a, Xihan Chen a, Zhuohang Li a, Feng Gao a b, Weixing Chen a b, Dual-function flapping hydrofoil: Energy capture and propulsion in ocean waves, Volume 222, February 2024, 119956
3. Fang Li, Qiaogao Huang, Guang Pan, Yao Shi, Effect of hydrofoil leading edge waviness on hydrodynamic performance and flow noise, Volume 231, 1 July 2021, 108883
4. Callum Stark, Weichao Shi, Moritz Troll, Cavitation funnel effect: Bio-inspired leading-edge tubercle application on ducted marine propeller blades, Volume 116, November 2021, 102864
5. Callum Stark, Weichao Shi, Mehmet Atlar, A numerical investigation into the influence of bio-inspired leading-edge tubercles on the hydrodynamic performance of a benchmark ducted propeller, Volume 237, 1 October 2021, 109593
6. S.M.A. Aftab a, N.A. Razak b, A.S. Mohd Rafie a, K.A. Ahmad , Mimicking the humpback whale: An aerodynamic perspective, Volume 84, July 2016, Pages 48-69
7. Anupam Krishnan, Abdulkareem Sh. Mahdi Al-Obaidi, A comprehensive review of innovative wind turbine airfoil and blade designs: Toward enhanced efficiency and sustainability, Volume 60, December 2023, 103511